MANAGEMENT SCIENCE
doi 10.1287/mnsc.1070.0787ec
pp. ec1–ec30

e-companion

ONLY AVAILABLE IN ELECTRONIC FORM

Electronic Companion—"Heterogeneity and Network Structure in the Dynamics of Diffusion: Comparing Agent-Based and Differential Equation Models" by Hazhir Rahmandad and John Sterman, *Management Science*, doi 10.1287/mnsc.1070.0787.

This supplement documents the DE and AB models and results, including the construction of the different networks for the AB simulations, sensitivity analysis, the calibration process and results, and instructions for simulating the model and replicating the results. The model, implemented in the Anylogic simulation environment, is available at: http://web.mit.edu/hazhir/www/research.html

EC.1. Formulation for the Agent-Based SEIR Model

We develop the agent based SEIR model and derive the classical differential equation model from it. Figure EC.1 shows the state transition chart for individual j. Individuals progress from Susceptible to Exposed (asymptomatic infectious) to Infectious (symptomatic) to Recovered (immune to reinfection). In the classical epidemiology literature the recovered state is often termed "Removed" to denote both recovery and cumulative mortality.

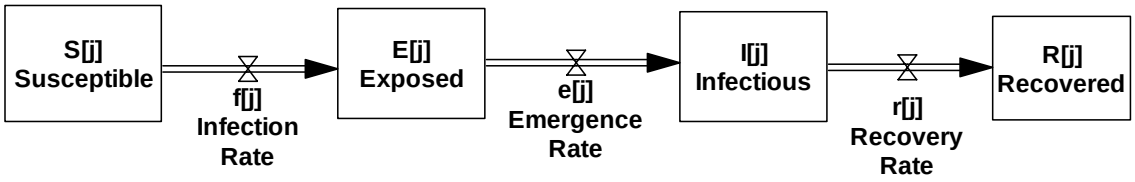

Figure EC.1 State Transitions for the AB SEIR model

The states SEIR are mutually exclusive; each individual in the AB model can only be in one of the states. We first derive the individual Infection Rate f[k] (the hazard of infection for a susceptible individual), then the Emergence and Recovery Rates e[j] and r[j] for individuals in the exposed and infectious states.

Infection Rate: For infection to occur Susceptible individuals must come into contact with either an Infectious or Exposed individual. Some of these contacts result in transmission of the infection. Infection (the transition from S to E) for susceptible individual k occurs if, first, the individual comes into contact with an individual j in either the E or I state, and second, that contact results in transmission of the infectious agent. The probability of contact between individual j and k in a short interval of time, dt, is denoted $C_{dt}[j,k]$. The probability of transmission from j to k given such a contact (infectivity) is denoted i_j.

Contacts between individuals occur with probabilities conditioned by the network of relationships in the population. Assuming contacts within the relationship network are independent events, the expected individual Infection Rate, f[k], can be found by summing the probabilities of contact with each individual in states E and I and finding the infectious contact hazard by taking the limit of the sum of infectious contact probabilities as the time interval dt approaches zero:

$$f[k]=\lim_{dt\to 0}\Big(\sum_{j\in EorI} C_{dt}[j,k]\cdot i_j\Big)/dt=\sum_{j\in EorI}\Big(\lim_{dt\to 0}((C_{dt}[j,k]\cdot i_j)/dt)\Big)=\sum_{j\in EorI}(Z[j,k]) \quad \text{(EC.1)}$$

In the following section we find the expected infectious contact rate between individuals j and k, Z[j,k], by deriving the formulations for its components based on the implementation of the AB model in the paper.

In the agent-based model, contacts between each E or I individual and other individuals in the population occur through the network of relationships between them. Infection can only occur when these contacts are with an individual in state S. Therefore, $C_{dt}[j,k]$ is composed of two components: (1) The event that an individual j in the state E or I ($R_{dt,n}[j]$) has (n) contact(s), within dt, and (2) The probability that any of these (n) contacts is with individual k in the state S (P[j,k]):

$$C_{dt}[j,k]=\sum_{n=1}^{\infty} R_{dt,n}[j]\cdot(1-(1-P[j,k])^n) \quad \text{(EC.2)}$$

Contacts for an E or I individual are assumed independent random variables with stationary increments and therefore have a Poisson distribution with parameter L[j]:

$$R_{dt,n}[j]=\frac{(L[j]\cdot dt)^n\cdot e^{(-L[j]\cdot dt)}}{n!} \quad \text{(EC.3)}$$

$$L[j]=c_j\cdot H[j] \quad \text{(EC.4)}$$

where c_j, the base contact rate, equals c_{IS} or c_{ES} depending on whether individual j is in the E or I state, and H[j] is the heterogeneity factor for individual j (defined below).

When contact occurs, the probability individual j contacts an individual selected randomly from the N-1 others is:

$$\text{Probability(j contacting k| j has a contact)= P[j,k]=} \frac{\lambda[k]\cdot NW[k,j]/K[k]^{\tau}}{\sum_{i\in N}\lambda[i]\cdot NW[i,j]/K[i]^{\tau}} \qquad \text{(EC.5)}$$

where:

λ[j]: The individual heterogeneity factor. Set to 1 in the homogeneous scenarios. In the heterogeneous cases λ[j] is drawn from a uniform distribution U[0.25-1.75].

K[j]: The number of links individual j has in his or her network.

NW[i,j], the network link, is 1 if there is a link between individuals i and j and 0 if there is none, or if i=j. N is the set of all individuals in the population.

The parameter τ captures the time constraint on contacts. In the homogeneous scenarios τ = 1. The total time for contacts with others is fixed, so that individuals with more links have fewer chances of contact with each link, compensating for the heterogeneity created by differing degree distributions in different networks. In the heterogeneous scenarios τ = 0 so that the probability of contact through all links is constant: those with more links contact more people (on average).

The formulation ensures that contacts of the E or I individuals are distributed among other population members depending on their heterogeneity factor and their connectedness.

The overall heterogeneity factor for individual j, H[j], is defined to ensure (1) that contact frequencies capture heterogeneity among individuals, represented by λ[j]; (2) that individual contact frequencies depend on the number of links to each individual in the heterogeneous condition but are independent of link density in the homogeneous condition; and (3) that the mean contact frequency across the entire population remains (in expectation) equal to that in the differential equation model. Note that this formulation captures two types of heterogeneity. First, individual-level heterogeneity is captured through λ[j]: people with higher λ will have higher contact rates. Second, network-level heterogeneity considers how many connections an individual has and therefore how likely it is for that person to contact any of those connections. Consequently:

$$H[j]=\frac{\lambda[j]\cdot W[j]\cdot N}{K[j]^{\tau}\cdot W_N} \qquad \text{(EC.6)}$$

where:

W[j] is the weighted sum of links to individual j:

$$\sum_{i \in N} \lambda[i] \cdot NW[i, j] / K[i]^{\tau} , \tag{EC.7}$$

and W_N, the population level weighted sum of W, normalizes H[j] so that the expected value of mean contacts equals the value in the DE model.

Hence

$$W_N = \sum_{N} \frac{\lambda[i] \cdot W[i]}{K[i]^{\tau}} . \tag{EC.8}$$

Finally, i_j, the probability of transmission given a contact between infectious individual j and susceptible k equals i_{ES} or i_{IS} depending on whether individual j is in the E or I state.

Therefore we can find the infectious contact rate between an individual k in state S and individual j in state E or I, Z[j,k], by substituting its components. Specifically, from eq. EC.1,

Z[j,k] is defined as $\lim_{dt \to 0} ((C_{dt}[j,k] \cdot i_j / dt))$

and from eq. EC.2 we have $C_{dt}[j,k] = \sum_{n=1}^{\infty} R_{dt,n}[j] \cdot (1 - (1 - P[j,k])^n)$, giving

$$Z[j,k] = \lim_{dt \to 0} ((C_{dt}[j,k] \cdot i_j) / dt) = \lim_{dt \to 0} ((\sum_{n=1}^{\infty} R_{dt,n}[j] \cdot (1 - (1 - P[j,k])^n) \cdot i_j) / dt) . \tag{EC.9}$$

Substituting *R[j]* , *P[j,k]* and their components from equations EC.3-EC.8, we find *Z[j,k]* in terms of the model parameters and variables (individual contact rates, infectivities, heterogeneity factors, and network structure),

$$Z[j,k] = \left(\frac{|N|}{\sum_{i,l} \frac{NW[i,l] \cdot \lambda[i] \cdot \lambda[l]}{(K[i] \cdot K[l])^{\tau}}} \right) \frac{NW[j,k] \cdot \lambda[j] \cdot \lambda[k]}{(K[j] \cdot K[k])^{\tau}} \cdot c_j \cdot i_j \tag{EC.10}$$

yielding the infection hazard for individual k in the state S:

$$f[k] = \sum_{j \in E,I} Z[j,k] . \tag{EC.11}$$

Emergence and Recovery: The DE SEIR model assumes populations within each state are well mixed. Consider the recovery process (emergence is analogous). Perfect mixing implies that the hazard rate of recovery for an infectious individual (the transition from I to R) depends only on the expected duration of the infectious phase, 1/δ, and is independent of how long that particular individual has been in the I state. Consequently residence times for infectious individuals are distributed exponentially. In the AB model, the duration of the infectious stage for infectious individual j is randomly drawn from the exponential distribution with mean duration 1/δ. Hence the hazard rate for recovery is r[j] = δ. Emergence (the transition from E to I) is formulated analogously, so e[j] = ε, where ε is the hazard rate for emergence.

EC.2. Deriving the deterministic compartment (differential equation) model

Figure EC.2 shows the structure of the deterministic compartment DE model.

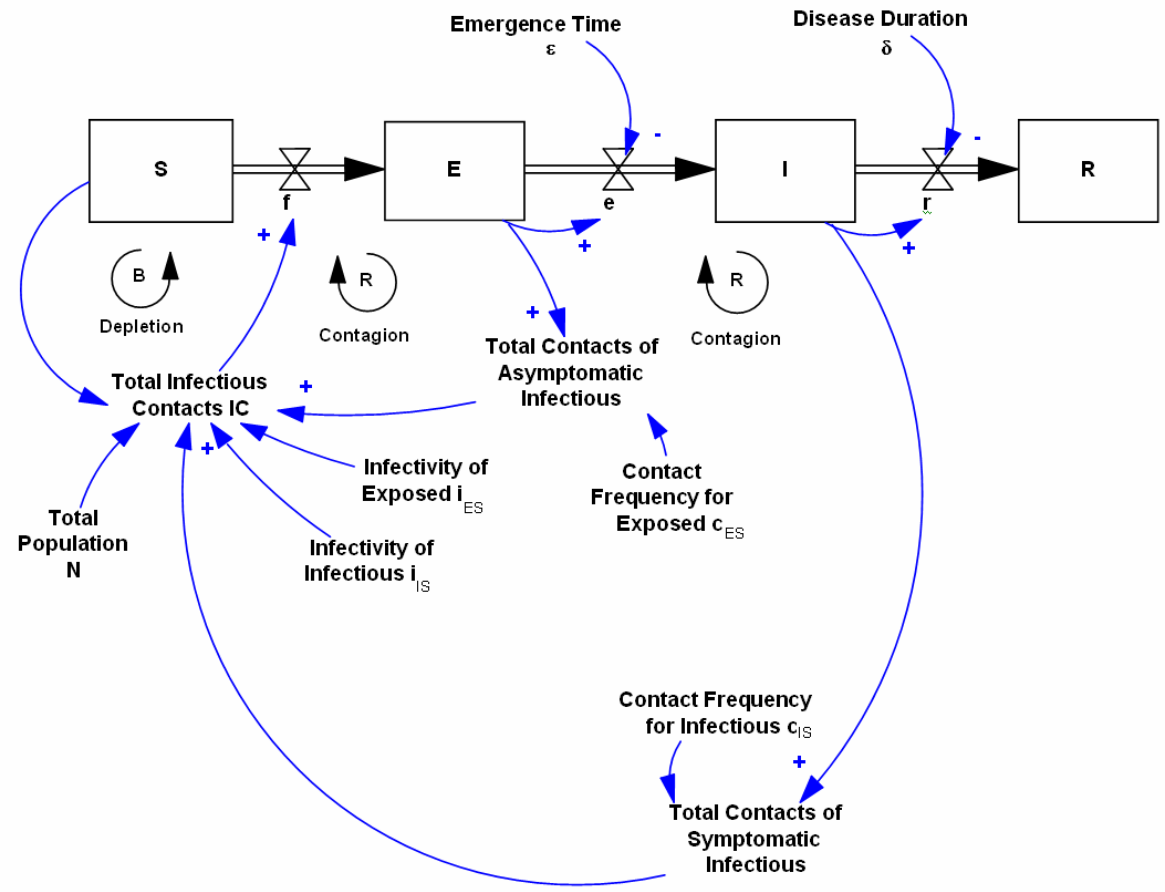

Figure EC.2 The structure of the SEIR differential equation model.

The deterministic compartment model can be derived from the underlying stochastic agent-based model by assuming (1) homogeneity of all individuals; (2) perfect mixing within compartments; and (3) the rates for the DE model are equated with the infinitesimal transition rate of the underlying stochastic transmission model.

To derive the DE formulation for the infection rate, f_{DE}, sum the individual infection rates f[j]:

$$f_{DE} = \sum_{J} f[j] = \sum_{J}\sum_{K} Z[j,k]. \quad \text{(EC.12)}$$

Homogeneity implies all individuals have the same number of links, K[j] = K[k] = K, and the same propensity to use their links, λ[j] = λ[k] = 1. Therefore:

$$Z[j,k] = \frac{c_j \cdot i_j \cdot N \cdot NW[j,k]}{\sum_{k,j} NW[j,k]}. \quad \text{(EC.13)}$$

NW[j,k] depends on the network structure. However, in the DE model individuals are assumed to be well mixed, implying everyone is linked to everyone else. Therefore

$$NW[j,k] / \sum_{k,j} NW[j,k] = 1/|N|^2 \quad \text{(EC.14)}$$

yielding

$$Z[j,k] = \frac{c_j \cdot i_j}{|N|}. \quad \text{(EC.15)}$$

Noting that homogeneity implies contact frequencies and infectivities are equal within states ($c_j = c_{ES}$ and $i_j = i_{ES}$ for all E and c_{IS} and $i_j = i_{IS}$ for all I) and substituting into the equation for the infection rate yields:

$$f_{DE} = \sum_{k\in S}\sum_{j\in E\vee I} \frac{c_j . i_j}{|N|} = \frac{1}{|N|}\sum_{k\in S}\left(\sum_{j\in E} c_{ES} . i_{ES} + \sum_{j\in I} c_{IS} . i_{IS}\right) \quad \text{(EC.16)}$$

which simplifies into the formulation for the infection rate in the DE model:

$$f_{DE} = (c_{ES} \cdot i_{ES} \cdot |E| + c_{IS} \cdot i_{IS} \cdot |I|) \cdot (|S|/|N|). \quad \text{(EC.17)}$$

The aggregate emergence and recovery rates in the DE are the sum of the expected individual emergence and recovery rates:

$$e_{DE} = \sum_{j \in E} E(e[j]) = \sum_{j \in E} \varepsilon = |E|\varepsilon \quad \text{and} \quad r_{DE} = \sum_{j \in I} E(r[j]) = \sum_{j \in I} \delta = |I|\delta \tag{EC.18}$$

which is the formulation for a first-order exponential delay with hazard rates ε and δ, respectively. The full SEIR model is thus:[1]

$$\frac{dS}{dt} = -f\,,\ \frac{dE}{dt} = f - e\,,\ \frac{dI}{dt} = e - r \tag{EC.19}$$

$$f = (c_{ES} \cdot i_{ES} \cdot E + c_{IS} \cdot i_{IS} \cdot I)(S/N) \tag{EC.20}$$

$$e = \varepsilon E \tag{EC.21}$$

$$r = \delta I \tag{EC.22}$$

EC.3. Network Structure

The connected and lattice networks are deterministic and hence the same in each AB simulation. The random, scale free, and small world networks are stochastic. Each AB simulation of these networks uses a different realization drawn from the appropriate network distribution. We assume, for each realization, a fixed network (FN) model: the structure of each network remains unchanged over the time horizon of the simulations. Moving from an FN to dynamic network in which arcs among nodes change over the time horizon of the epidemic, either exogenously or endogenously, would introduce additional mixing. The details of construction for each network follow.

Connected: every node is connected to every other node.

[1] Note that in the derivation of the individual-level AB model, the symbols S, E, I and R denote the sets of individuals in the susceptible, exposed, infectious and removed states, respectively (with, e.g., |E| denoting the number of exposed individuals in the set E, while, consistent with standard practice, in the DE model (eq. 19-22), S, E, I and R are continuous, real-valued state variables representing the number of people in each state rather than the set of individuals in each state.

Random: The probability of a connection between nodes i and j is fixed, p=k/(N-1), where k is the average number of links per person. In the base case k = 10 and N = 200. In the sensitivity analysis over population size, k = 6 and 18 when N = 50 and 800, respectively.

Scale-free: Barabasi and Albert (1999) outline the preferential attachment algorithm to grow scale-free networks. The algorithm starts with m_0 initial nodes and adds new nodes one at a time. Each new node is connected to previous nodes through m new links, where the probability each existing node j receives one of the new links is m*K[j]//ΣK[j] where K[j] is the number of links into node j. The probability that node j has connectivity smaller than k after t time steps is then:

$$P(K[j]_t<k) = 1 - m^2t/(k^2(t + m_0)) \quad \text{(EC.23)}$$

We use the same procedure with $m = m_0 = k$ (the average number of links per person). Following the original paper (Albert 2005, personal communication), we start with m_0 individuals connected to each other in a ring, and then add the rest of the $N - m_0$ individuals to the structure. The model accompanying the online material includes the Java code used to implement all networks.

Small World: Following Watts and Strogatz (1998), we build the small world network by ordering all individuals into a one-dimensional ring lattice in which each individual is connected to the k/2 closest neighbors. Then we rewire these links to a randomly chosen member of the population with probability p = 0.05

Ring Lattice: In the ring lattice each node is linked to the k/2 nearest neighbors on each side of the node (equivalent to the small world case with zero probability of long-range links.)

EC.4. Histogram of Final Size for each network and heterogeneity condition

Histograms for the fraction of the population ultimately infected (final size, F) are shown in Figure EC.3 for each network and heterogeneity condition. The heterogeneous cases are shown in blue and homogeneous cases in red.

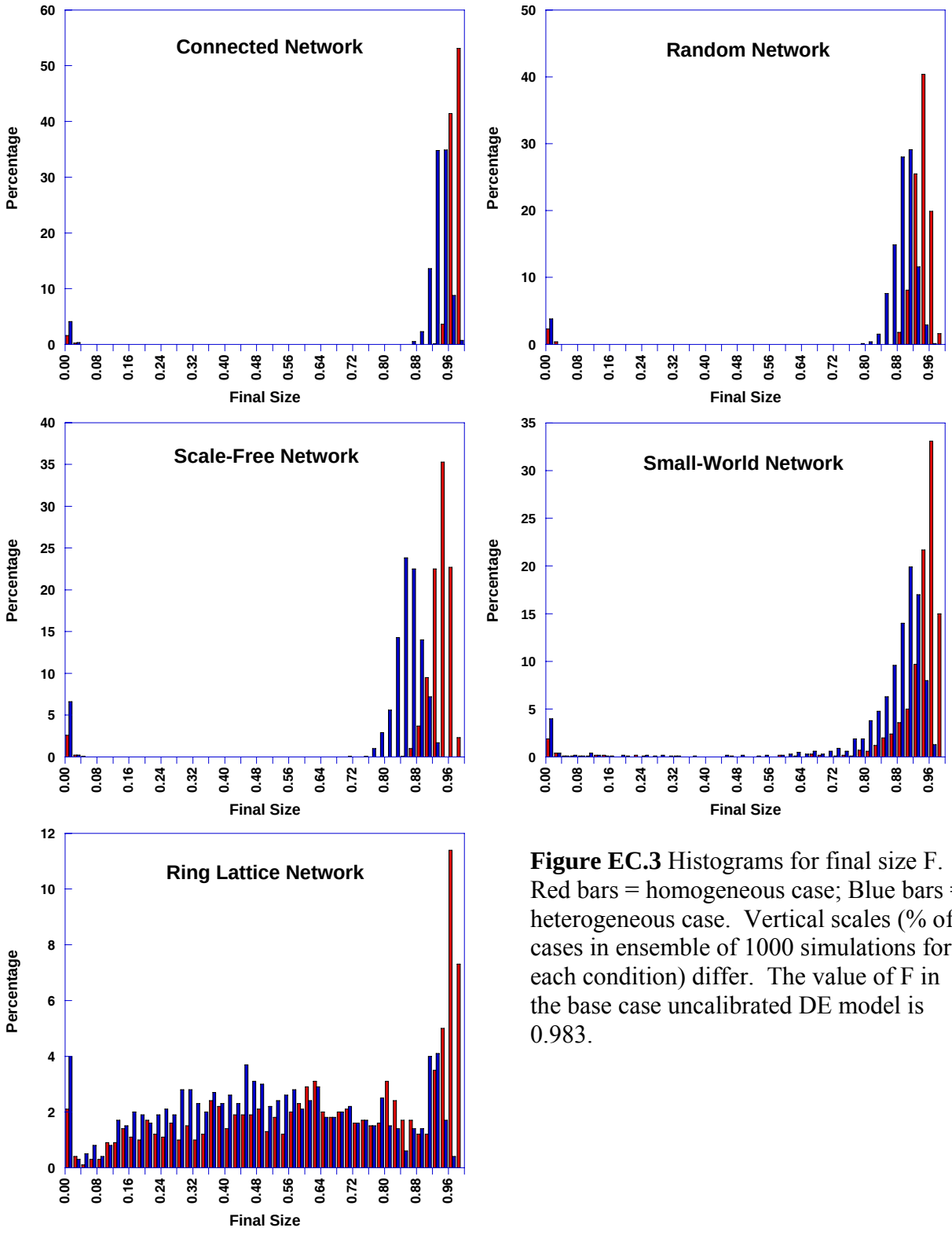

Figure EC.3 Histograms for final size F. Red bars = homogeneous case; Blue bars = heterogeneous case. Vertical scales (% of cases in ensemble of 1000 simulations for each condition) differ. The value of F in the base case uncalibrated DE model is 0.983.

EC.5. The Calibrated DE Model

We calibrate the DE model to the trajectory of the infectious population in 200 randomly selected simulations from each of the ten AB scenarios (5 networks x 2 heterogeneity conditions). The best-fit parameters for both infectivities (i_{ES} and i_{IS}) and for the duration of the incubation phase ($1/\varepsilon$) are estimated by minimizing the sum of squared error between the recovered population in the AB simulation, R_{AB}, and the recovered population in the DE model, R_{DE}, from the start of the simulation through time T, subject to the DE model structure:

$$\min_{i_{ES}, i_{IS}, 1/\varepsilon} \sum_{t=0}^{T} [R_{DE}(t) - R_{AB}(t)]^2 \qquad \text{(EC.24)}$$

We use the Vensim™ software optimization engine for the estimation.[2]

The interval T is selected to capture the full lifecycle of the epidemic. Diffusion is faster in the connected, random, and scale-free cases, so T = 300 days. Diffusion is slower in the small world and lattice networks, so T = 500 days. The estimated parameters are constrained such that $0 \le i_{ES}$, i_{IS} and $0 \le 1/\varepsilon \le 30$ days.

Table EC.1 shows the calibration results, including the median and standard deviation for each parameter, the implied value of R_0, and the goodness of fit (R^2) for each of the ten scenarios. Also reported are the correlations among the three estimated parameters. The correlation matrix could be used to create joint parameter distributions consistent with each network and heterogeneity condition as the basis for monte-carlo simulations of the DE model that would approximate the variability generated by each network and heterogeneity condition in the stochastic AB model. Further work is needed to test this idea. Table EC.2 shows how well the trajectory of the calibrated DE model matches the AB models for the three metrics examined here, including final fraction infected, peak time, and peak prevalence.[3]

---

[2] We chose not to estimate the mean duration of disease, $1/\delta$, because it is more likely to be constrained by clinical data than the incubation period and infectivities. Estimating $1/\delta$ would further improve the ability of the DE to fit the realizations of the AB model by adding another important degree of freedom to the estimation.

[3] Other metrics may be relevant depending on model purpose. These include R_0 (which, however, is strongly related to F), and the cost/benefit ratio for different policies (which depend on the particular disease and other situation-specific parameters). If data are available for a particular setting then the models and comparison procedure used here can be applied to assess differences between the AB and DE models and whether those differences are large or small relative to variation in outcomes arising from stochastic events, parameter uncertainty, feedbacks affecting individual behavior, model boundary, etc.

Tables EC.1 and EC.2 show three main results: First, the calibrated DE models fit the AB dynamics well in all network and heterogeneity conditions and for all metrics we examine (median $R^2 \geq 0.985$ in all conditions). Second, there is considerable variation in the estimated parameters for each realization within a given network and heterogeneity condition. Third, for all but the homogeneous fully connected case, the median estimates of the parameters, including the implied value of R_0, are biased compared to the underlying values.

To gain insight into why the deterministic compartment model captures the results of the stochastic AB model even when its mixing and homogeneity assumptions are violated, note that in deterministic SEIR compartment models, R_0 is related to final size by $R_0 = -\ln(1 - F)/F$ (Anderson and May 1991). In the compartment model here, $R_0 = c_{ES}i_{ES}/\varepsilon + c_{IS}i_{IS}/\delta$. Therefore, when the value of F in a realization of the AB model differs from the base case of the DE, the estimated values of the transmission rates $c_{ES}i_{ES}$ and $c_{IS}i_{IS}$ and the incubation period $1/\varepsilon$ will differ compared to their base values to yield the R_0 implied by the value of F in that realization. Within the constraint given by $-\ln(1 - F)/F = c_{ES}i_{ES}/\varepsilon + c_{IS}i_{IS}/\delta$, the timing of the epidemic, specifically the inflection point in cumulative cases, is then captured by the values of the incubation time $1/\varepsilon$ and transmission rates $c_{ES}i_{ES}$ and $c_{IS}i_{IS}$ that yield the best fit (slower diffusion, given a value of F, implies longer incubation times with correspondingly lower transmission rates). Matching the timing and slope of cumulative cases at the inflection point yields a good estimate of the peak time T_p and maximum prevalence I_{max}: the inflection point in cumulative cases occurs when the infection rate r is at its maximum because $dR/dt = r$. But $r = \delta I$, so the inflection point in R occurs when I is at its maximum, which, by definition, is the point (T_p, I_{max}).[4]

To understand the wide variation in estimated parameters within a network and heterogeneity condition, consider the homogeneous fully connected case. This condition corresponds to the mixing and homogeneity assumptions of the DE model; the only difference between the DE and

[4] The fit between the DE and AB models is better for F, on average, than the fit for T_p and I_{max} because the timing and value of peak prevalence are subject to more random variation in the AB model than the final fraction afflicted. Cumulative cases is the product of the final fraction infected, F, and population, N, $FN = \int_0^\infty rdt = \int_0^\infty edt$, while prevalence at time T is given by $I_T = \int_0^T (e - r)dt$. Since the emergence and recovery flows e and r are subject to stochastic variation, the integral of their difference at any moment in time, and therefore the timing and maximum value of I, will typically be more variable than their common cumulative value at the end of the epidemic.

the $H_{=}$ fully connected AB model is that the AB model treats discrete individuals with stochastic transitions between states rather than the continuous real-valued states and deterministic state transitions of the DE. As shown in Table EC.1, the median parameter estimates for the $H_{=}$ connected AB model are close to the true values (the median $R_0 = 4.21$ vs. the true value of 4.125). However, even when the mixing and homogeneity assumptions of the DE are satisfied there is still considerable variation in the parameter estimates for the individual realizations: the standard deviation in the estimated values of $R_0 = 1.71$. In cases where, by chance, fewer contacts are realized than expected, the epidemic will be milder than expected and the realized value of F smaller than the mean value (see Figure EC.3). To satisfy $R_0 = -\ln(1 - F)/F$, lower F requires that the estimated parameters adjust to yield lower R_0. In a realization with low F, the low estimate of R_0 is quite different from the expected value, but is the best estimate of the basic reproduction rate for that particular epidemic, in which, by chance, transmission was in fact lower than expected. Thus the large spread in the estimated parameters within a given network and heterogeneity condition reflects the wide range of outcomes in the stochastic AB model.

To understand the third phenomenon (biased estimates in conditions other than the H= connected case), recall that heterogeneity and clustering lead to lower average values for F (Table 3 in the paper), which then forces the average value of R_0 down via $R_0 = -\ln(1 - F)/F$. Therefore, when the mixing and heterogeneity assumptions of the DE are violated, the average estimates of transmission rates and incubation time, and hence R_0, will be biased.

The parameter values obtained by fitting the aggregate model to the data from an AB simulation (and therefore from the real world) not only capture the mean of individual attributes such as contact rates but also the impact of heterogeneity and network structure. When the network structure and degree of individual heterogeneity in the actual situation differ from the assumptions of the estimated model (whether DE or AB), the estimated model will be misspecified and the parameter estimates biased. Modelers often use both micro-level and aggregate data to parameterize both AB and DE models. The estimation results suggest caution must be exercised in doing so, and in comparing parameter values across different models (Fahse et al. 1998). Note also that the ability to reproduce historical data does not imply that calibrated compartment models will respond to policies the same way the AB models do (Table EC.8).

Parameter		Connected		Random		Scale-free		Small World		Lattice	
		$H_=$	$H_\neq$	$H_=$	$H_\neq$	$H_=$	$H_\neq$	$H_=$	$H_\neq$	$H_=$	$H_\neq$
Infectivity of Exposed i_{ES}	Median	0.045	0.053	0.044	0.049	0.034	0.065	0.025	0.026	0.025	0.040
	σ	0.021	0.088	0.023	0.171	0.093	0.245	0.055	0.135	0.280	0.310
Infectivity of Infectious i_{IS}	Median	0.100	0.025	0.047	0.081	0.081	0.061	0.050	0.015	0.023	0.015
	σ	0.115	0.067	0.068	0.058	0.068	0.048	0.076	0.060	0.037	0.032
Average Incubation Time $1/\varepsilon$	Median	14.46	10.87	12.13	6.73	12.43	3.61	21.21	16.47	6.80	3.50
	σ	4.57	5.14	4.88	5.32	5.43	4.66	7.81	8.53	13.05	10.70
Implied $R_0 = c_{ES}*i_{ES}/\varepsilon + c_{IS}*i_{IS}/\delta$	Median	4.21	2.96	3.10	2.54	3.15	2.27	3.35	2.54	1.61	1.35
	σ	1.71	0.62	0.58	0.52	0.66	0.64	0.88	0.66	0.81	0.55
R^2	Median	0.999	0.999	0.999	0.999	0.999	0.999	0.998	0.998	0.985	0.987
	σ	0.025	0.049	0.017	0.050	0.016	0.039	0.040	0.059	0.056	0.043
Correlations	i_{ES}, i_{IS}	-0.70	-0.08	-0.80	0.16	-0.29	0.48	-0.30	-0.19	0.04	0.19
	i_{ES}, $1/\varepsilon$	0.61	-0.20	0.54	-0.40	-0.08	-0.53	-0.21	-0.25	-0.49	-0.46
	i_{IS}, $1/\varepsilon$	-0.31	-0.75	-0.73	-0.80	-0.53	-0.71	-0.17	-0.33	-0.06	-0.34

Table EC.1 Median and standard deviation, σ, of estimated parameters for the calibrated DE model. Reports results of 200 randomly selected runs of the AB model for each cell of the experimental design. Compare to base case parameters $i_{ES} = 0.05$, $i_{IS} = 0.06$, $1/\varepsilon = 15$ days. The median and standard deviation of the basic reproduction number, $R_0 = c_{ES}i_{ES}/\varepsilon + c_{IS}i_{IS}/\delta$, computed from the estimated parameters, is also shown. The table also shows the correlations among the different estimated parameters in each network and heterogeneity setting.

Metric	Conf. Bound	Connected		Random		Scale-free		Small World		Lattice	
		$H_=$	$H_\neq$	$H_=$	$H_\neq$	$H_=$	$H_\neq$	$H_=$	$H_\neq$	$H_=$	$H_\neq$
Final Size	95%	99.5	94	96	95.5	90	87.5	97.5	91.5	96	95
	90%	95.5	89.5	88.5	89	87	84.5	89.5	87.5	90	89.5
Peak Time, T_p	95%	97	93.5	95.5	91.5	93.5	93.5	96	93.5	89.5	93
	90%	95	88.5	90	86.5	91.5	89.5	94.5	87.5	85.5	79.5
Peak Prev, I_{max}	95%	97.5	96.5	97.5	95.5	97.5	98.5	97	98	94	95.5
	90%	92.5	93.5	89.5	83.5	86	93.5	92	91.5	75.5	85

Table EC.2 The percentage of the 200 fitted DE simulations falling inside the 95% and 90% confidence intervals defined by the ensemble of AB simulations for Final Size, Peak Time, and Peak Prevalence, under each network and heterogeneity condition.

EC.6. Sensitivity to population size

To investigate the sensitivity of the results to population size, we repeat the analysis for populations of 50 and 800 individuals (± a factor of 4 from the base case)[5]. For each population we run 1000 simulations for each network and heterogeneity condition. Table EC.3 reports mean and standard deviation of each metric for each population size. Values of each metric in the base case DE model are shown in parentheses under each metric name (left column). */** indicates the DE simulation falls outside the 95/99% confidence bound defined by the ensemble of AB simulations.

In the N = 50 case, the uncalibrated DE values of T_p and I_{max} fall within the range capturing 95% of the AB realizations in all network type and heterogeneity conditions. In the N = 800 case, the uncalibrated DE values of T_p fall within the range capturing 95% of the AB realizations in all cases except the $H_=$ small world case, which falls within the 99% range. The DE values of I_{max} under N = 800 fall within the 95% range for all cases except the small world and lattice (both $H_=$ and $H_{\neq}$). In the N = 50 case, the DE values of F fall within the 95% range of AB realizations for all homogenous network conditions, and within the 99% range for all heterogeneous conditions. In the N=800 case, the DE values of F generally fall outside the interval capturing 95% of the AB realizations, with better fit for the $H_=$ than $H_{\neq}$ cases. Nevertheless, note that the mean value of F in the N = 800 case across all conditions is 87.3%, much closer to the DE value of 98.3% than the mean of 80.1% in the N = 50 case.

In sum the results are generally robust to population size. Across populations varying by a factor of 16, the peak burden on public health resources and the time available to policymakers to deploy those resources in the deterministic compartment model fall within the envelope encompassing 95% of the AB realizations in most conditions, the primary exception again being the lattice. Also like the N = 200 case, cumulative prevalence in the DE is higher than in the AB models and tends to fall outside the 95% outcome interval, particularly for the heterogeneous cases. As population changes we observe what is predicted in theory, specifically that an increase in population reduces the variability of results, so that the population of 50 has larger confidence intervals in the AB simulations. This is expected as the impact of stochastic events and the dif-

[5] Mean links per node (k) must be scaled along with population. We use the scaling scheme that preserves the average distance between nodes in the random network (Newman 2003), yielding k=6 and k=18 for N=50 and N=800.

ference between the continuous flow assumptions of the DE model and the treatment of discrete individuals in the AB model should prove more important in smaller populations. Moreover, increased variability increases the peak prevalence for smaller populations since the maximum of the symptomatic population, a random variable, grows with increased variability.

Population N=800		Connected		Random		Scale-free		Small World		Lattice	
		$H_=$	$H_\neq$	$H_=$	$H_\neq$	$H_=$	$H_\neq$	$H_=$	$H_\neq$	$H_=$	$H_\neq$
Final Size (0.983)	Mean	**0.95**	**0.90****	**0.94***	**0.88****	**0.94****	**0.82****	**0.95**	**0.89****	**0.82**	**0.64****
	σ	**0.17**	**0.18**	**0.15**	**0.17**	**0.16**	**0.20**	**0.14**	**0.18**	**0.24**	**0.27**
	% F < 0.1	**3.1**	**3.9**	**2.4**	**3.5**	**2.7**	**5.6**	**2.1**	**3.9**	**2.2**	**4.8**
Peak Time, T_p (57.2)	Mean	**58.2**	**51.9**	**61.4**	**55.6**	**66.4**	**46**	**99.6***	**87.6**	**153.8**	**130**
	σ	**12.4**	**12.4**	**13.1**	**12.9**	**14.2**	**13.4**	**22.4**	**23.4**	**123.7**	**101.9**
Peak Prev., I_{max} (27%)	Mean	**27**	**25.9**	**26**	**24.6**	**24.9**	**23.5**	**18.8****	**18.2****	**5.4****	**5.0****
	σ	**5**	**5.4**	**4.3**	**4.9**	**4.1**	**5.9**	**3.4**	**4.1**	**1.6**	**1.7**

Population N=50		Connected		Random		Scale-free		Small World		Lattice	
		$H_=$	$H_\neq$	$H_=$	$H_\neq$	$H_=$	$H_\neq$	$H_=$	$H_\neq$	$H_=$	$H_\neq$
Final Size (0.983)	Mean	**0.96**	**0.90**	**0.89**	**0.81***	**0.85**	**0.80***	**0.80**	**0.70***	**0.70**	**0.60***
	σ	**0.14**	**0.17**	**0.17**	**0.21**	**0.22**	**0.20**	**0.25**	**0.27**	**0.28**	**0.27**
	% F < 0.1	**2.1**	**3.5**	**3.2**	**5.5**	**3.3**	**5.8**	**2.8**	**4.7**	**3**	**3.8**
Peak Time, T_p (37.8)	Mean	**39.92**	**37.89**	**42.99**	**40.36**	**48.9**	**38.5**	**51.26**	**47.99**	**48.52**	**46.86**
	σ	**12.43**	**13.17**	**16.13**	**16.98**	**21.1**	**16.9**	**26.71**	**27.2**	**28.68**	**30.05**
Peak Prev., I_{max} (27.5[6])	Mean	**33.2**	**31.4**	**29.3**	**27**	**25.9**	**27**	**22.1**	**20.3**	**18.9**	**17.3**
	σ	**7.29**	**7.85**	**7.47**	**8.18**	**8.21**	**7.99**	**7.85**	**7.94**	**7.11**	**6.75**

Table EC.3 Results for populations of 50 and 800.

EC.7. Sensitivity to R_0

We vary R_0 from half to double the base case value by scaling the contact frequencies for the E and I populations equally. Specifically, the low case gives $c_{ES} = 2$ and $c_{IS} = 0.625$ yielding $R_0 = 2.0625$, and the high case gives $c_{ES} = 8$ and $c_{IS} = 2.5$, yielding $R_0 = 8.25$. We repeat the base case analysis with these parameter settings. Table EC.4 reports the mean and standard deviation

[6] Note that values of T_p and I_{max} in the DE depend on population N. The course of the epidemic depends on the initial fraction of the population susceptible to infection. All simulations begin with 2 randomly selected individuals in the emergence phase, and therefore N – 2 susceptibles. Hence the susceptible fraction of the population is initially 96% (48/50) when N = 50 and 99.75% (798/800) when N = 800.

for the three metrics for each value of R_0. Values of each metric in the base case DE model are shown in parentheses under each metric name (left column). */** indicates the DE simulation falls outside the 95/99% confidence bound defined by the ensemble of AB simulations.

Sensitivity: $R_0 = 2.0625$		Connected		Random		Scale-free		Small World		Lattice	
		$H_=$	$H_{\neq}$	$H_=$	$H_{\neq}$	$H_=$	$H_{\neq}$	$H_=$	$H_{\neq}$	$H_=$	$H_{\neq}$
Final Size, F (0.814)	Mean	**0.68**	**0.65**	**0.56**	**0.53****	**0.54***	**0.52****	**0.25****	**0.21****	**0.13****	**0.12****
	σ	**0.30**	**0.28**	**0.30**	**0.28**	**0.29**	**0.26**	**0.21**	**0.20**	**0.10**	**0.09**
	% F < 0.1	**16.4**	**15.9**	**22.1**	**21.8**	**22**	**20.7**	**31.7**	**39.7**	**43.7**	**46.4**
Peak Time, T_p (93.7)	Mean	**85.8**	**72.0**	**87.2**	**76.7**	**66.5**	**61.9**	**76.8**	**65.1**	**51.9**	**47.9**
	σ	**44.6**	**35.6**	**51.7**	**44.4**	**37.5**	**34.5**	**64.4**	**57.6**	**41.0**	**35.8**
Peak Prev., I_{max} (12.6%)	Mean	**26.4**	**27.9**	**20.6**	**21.8**	**24.2**	**24.4**	**9.2***	**8.7***	**6.6****	**6.5****
	σ	**12.3**	**12.7**	**11.5**	**11.7**	**13.0**	**12.6**	**5.5**	**5.9**	**3.6**	**3.5**

Sensitivity: $R_0 = 8.25$		Connected		Random		Scale-free		Small World		Lattice	
		$H_=$	$H_{\neq}$	$H_=$	$H_{\neq}$	$H_=$	$H_{\neq}$	$H_=$	$H_{\neq}$	$H_=$	$H_{\neq}$
Final Size, F (0.9997)	Mean	**1.00**	**0.98**	**0.99**	**0.97****	**0.98**	**0.94****	**1.00**	**0.98**	**0.99**	**0.96**
	σ	**0.04**	**0.09**	**0.06**	**0.06**	**0.07**	**0.12**	**0.05**	**0.08**	**0.07**	**0.12**
	% F < 0.1	**0.2**	**0.8**	**0.4**	**0.4**	**0.5**	**1.6**	**0.3**	**0.7**	**0.4**	**0.5**
Peak Time, T_p (29.6)	Mean	**30.7**	**29.9**	**32.5**	**32.3**	**30.6**	**30.3**	**45.4***	**45.3***	**65.0***	**67.8***
	σ	**4.9**	**5.5**	**5.6**	**6.0**	**5.8**	**6.9**	**8.8**	**10.2**	**26.7**	**29.7**
Peak Prev., I_{max} (34.2%)	Mean	**36.2**	**34.8**	**34.9**	**33.3**	**34.5**	**32.4**	**31.2**	**29.5**	**19.6****	**18.0****
	σ	**3.4**	**4.2**	**3.7**	**3.6**	**3.7**	**4.9**	**3.9**	**4.2**	**4.4**	**4.4**

Table EC.4 Sensitivity to R_0

In the low R_0 case, the base DE value of T_p falls within the range capturing 95% of the AB realizations in all networks and heterogeneity conditions. In the high R_0 case, the base value of T_p falls within the 95% interval for the connected, random, and scale free networks, and within the 99% interval for the small world and lattice. Higher R_0 reduces the incidence of early quenching, reducing the width of the interval capturing 95% of the AB outcomes. In the low R_0 case, the base DE value of I_{max} falls within the 95% interval for the connected, random, and scale free cases, within the 99% interval for the small world case, and outside the 99% interval for the lattice. In the high R_0 case, the base DE value of I_{max} falls inside the 95% interval for all conditions except the lattice. In the low R_0 case, the DE value of F falls outside the 95% interval

of AB realizations in all cases except the connected and $H_{=}$ random network. In the high R_0 case the DE value of F falls inside the 95% interval for all cases except the heterogeneous conditions of the random and scale free networks, even though the standard deviation of F in these cases is much smaller than in the low R_0 cases.

EC.8. Sensitivity to Disease Natural History

In reality, the infectivity of an infected individual varies over time. Typically, infectivity is initially zero, gradually rises, and finally wanes as the individual recovers. In many cases, individuals become infectious before becoming symptomatic. One way to capture time-varying infectivity is to add additional compartments to the E and I states, each with a potentially different infectivity, with the number of additional compartments large enough to approximate the distribution of infectivity well enough for the purpose. Here, we maintain the four compartment structure of the SEIR model and capture the possibility that late-stage incubating individuals become infectious by allowing $0 < i_{ES} < i_{IS}$.

To examine the sensitivity of results to this assumption, we test the opposite extreme, where $i_{ES} = 0$, implying all exposed individuals remain uninfectious. We maintain the base case value of $R_0 = 4.125$ by changing the infectivities to $i_{ES} = 0$ and $i_{IS} = 0.22$ and keeping all the other parameters at the base value, ensuring that the only difference between the base case and this case is the distribution of infectivity between the E and I states. Table EC.5 reports the results. Values of each metric in the base case DE model are shown in parentheses under each metric name (left column). */** indicates the DE simulation falls outside the 95/99% confidence bound defined by the ensemble of AB simulations. Note that since we keep R_0 at its original base case value, the final size of the epidemic (98.3% of the population afflicted) remains the same. However, since a newly infected individual cannot infect others until later, the peak time is later; slower growth also lowers peak prevalence compared to the base case. Nevertheless, as in the base case, the DE value of T_p falls within the 95% interval of AB realizations in all network and heterogeneity conditions. Also as in the base case, the DE value of I_{max} falls within the 95% interval of outcomes for all cases except the small world and lattice networks. And as in the base case, the DE value of F falls outside the 95% interval in all $H_{\neq}$ conditions, with somewhat better

correspondence to the AB results in the $H_{=}$ conditions. Overall, assuming that exposed individuals are not contagious has little impact on the differences between the DE and the mean of the AB behavior relative to the variability in AB outcomes. Additional tests, beyond the scope of this paper, would be required to assess the robustness of these results to other possible assumptions about pre-symptomatic infectivity, such as in models where the exposed stage is disaggregated into additional compartments to capture realistic distributions for transmissibility as a function of time since infection.

Sensitivity: i_{ES}=0 and i_{IS}=0.22		Connected		Random		Scale-free		Small World		Lattice	
		$H_{=}$	$H_{\neq}$	$H_{=}$	$H_{\neq}$	$H_{=}$	$H_{\neq}$	$H_{=}$	$H_{\neq}$	$H_{=}$	$H_{\neq}$
Final Size (0.983)	Mean	**0.908**	**0.87****	**0.86***	**0.80****	**0.83****	**0.77****	**0.81**	**0.70****	**0.44***	**0.34****
	σ	**0.26**	**0.24**	**0.26**	**0.26**	**0.24**	**0.24**	**0.27**	**0.29**	**0.26**	**0.22**
	% F < 0.1	**7.6**	**7.3**	**8.2**	**9.6**	**8.2**	**9**	**7.9**	**11.5**	**9.4**	**14.4**
Peak Time, T_p (89.15)	Mean	**90.9**	**85.7**	**101.9**	**95.9**	**89.5**	**85.9**	**169.9**	**152.0**	**119.8**	**102.3**
	σ	**33.3**	**31.0**	**38.3**	**38.3**	**36.0**	**35.0**	**92.4**	**89.0**	**96.4**	**78.7**
Peak Prev., I_{max} (20%)	Mean	**20.9**	**20.8**	**17.7**	**16.6**	**18.3**	**17.1**	**9.3****	**8.5****	**5.1****	**4.6****
	σ	**6.5**	**6.4**	**5.8**	**5.9**	**6.1**	**5.9**	**3.7**	**3.9**	**2.1**	**2.1**

Table EC.5 Sensitivity to natural disease history

EC.9. Policy Analysis and Model Boundary

Contact reduction can result from at least two processes: (1) the introduction of mandatory policies such as quarantine, isolation and travel restrictions; and (2) voluntary social distancing in which individuals reduce their contacts out of fear of contracting the disease. The former is a policy initiated by officials; the latter an endogenous feedback effect. A given scenario for contact reduction can be interpreted as resulting from a mix of mandatory measures and voluntary social distancing feedback. Hence the contact reduction results provide an example not only of policy analysis but also of the impact of expanding the model boundary.

We assume that contact reduction is initiated when the cumulative number of confirmed cases detected rises above some threshold. Typically, the extent of social distancing and the scope of control policies—the number of people affected, and the stringency of restrictions on their movements—increases with cumulative confirmed cases, as documented for the SARS epi-

demic (Wallinga and Teunis 2004): As the epidemic grows, the broader will be the mandate for quarantine government officials will propose and society will accept. Further, the propensity of individuals to self-quarantine by staying away from work, school and other mixing sites increases with the perceived threat from the disease, thus reducing contact frequencies. In the following we denote these feedbacks as a "quarantine policy" though it is important to recognize that the reduction in contacts could result from mandatory measures, voluntary social distancing, or a mixture of both. We model these effects as a reduction in the frequency of contacts between infectious individuals j and susceptibles s, c_{js}. Specifically, contact frequencies fall linearly from initial levels c^*_{js} to the minimum rates achieved under contact reduction, c^q_{js}, as cumulative confirmed cases rise, according to equations (6-7) in the paper:

$$c_{js} = (1-q)c^*_{js} + qc^q_{js} \quad \text{(EC.25)}$$

$$q = MIN[1, MAX(0,(P-P_0)/(P_q-P_0))] \quad \text{(EC.26)}$$

where the intensity of the effect, q, rises linearly from zero to one as the number of confirmed cases (cumulative prevalence, P = E + I), rises from the implementation threshold, P_0, to the level at which contact reduction saturates, P_q. We set $P_0 = 2$ and $P_q = 10$ cases. Because mandatory measures and voluntary social distancing are never perfect (some contacts inevitably arise from infectious individuals who maintain some contacts or who violate quarantine, and from contact between the quarantined and health providers), the minimum contact frequency does not fall to zero. In the simulations here we set $c^q_{js} = 0.15c^*_{js}$.

Note that the policy examined here is a simple one in which the impact of growing prevalence on contact frequencies is uniform across all individuals. The AB models can be used to examine policies that take advantage of the network structure, if it is known or can be determined in real time as the epidemic unfolds, while such policies must be approximated in compartment models (as in Kaplan, Craft and Wein 2002, 2003). Further work would be needed to examine the differences between the DE and AB models for such network-dependent policies.

Figure EC.4 compares the results of the quarantine policy to the no-quarantine base case for the DE model. Figure EC.5 shows the first 90 days in more detail, showing that contact reduction begins around day 8 and reaches full implementation around day 18. As expected, contact

reduction dramatically shortens the epidemic and reduces cumulative cases. In the base DE model, F falls from 98% infected to 19%. The epidemic peaks after 31 days, compared to 48 days without quarantine, and with peak prevalence of infectious individuals of 4.4%, compared to 27% in the base case. Due to the incubation time the peak of the infectious population lags full implementation of contact reduction measures.

Note that the E and I populations decay quite slowly after full quarantine implementation. The slow decay is due to the assumption that quarantine is imperfect. In the simulation R_0 falls to a minimum of about 0.6 at full implementation. Consequently some new cases continue to be generated, lengthening the effective time constant for the decay of the infectious population.

Table 5 in the paper (repeated here as Table EC.6) compares T_p, I_{max}, and F in the AB models to the base DE case. The base DE values of T_p and I_{max} fall within the interval capturing 95% of the AB realizations in all network and heterogeneity conditions. The base DE value of F falls inside the 95% confidence interval for all cases except the lattice.

The impact of the policy on the public health metrics is large compared to the variability in the realizations of the individual AB simulations and in the variability of the metrics across network and heterogeneity conditions.

Metric		Connected		Random		Scale-free		Small World		Lattice	
		$H_=$	$H_{\neq}$	$H_=$	$H_{\neq}$	$H_=$	$H_{\neq}$	$H_=$	$H_{\neq}$	$H_=$	$H_{\neq}$
Final Size F	μ	0.215	0.249	0.157	0.201	0.148	0.247	0.112	0.117	0.102*	0.099*
	σ	0.084	0.091	0.064	0.088	0.062	0.105	0.044	0.048	0.037	0.035
Peak Time T_p	μ	35.0	36.1	33.1	34.6	34.1	34.9	30.3	30.5	29.4	30.4
	σ	15.3	15.9	14.8	16.7	15.7	18.1	13.5	14.2	13.5	14.6
Peak Prev I_{max}	μ	6.42	7.28	5.17	6.15	4.98	7.43	4.17	4.35	3.97	3.89
	σ	2.40	2.66	1.99	2.55	1.98	3.23	1.58	1.67	1.52	1.42

Table EC.6 Behavior of three public health metrics under the quarantine policy. */** indicates the value of the metric in the DE model falls outside the 95/99% confidence bound defined by the ensemble of AB simulations. The results for the DE model under quarantine are F = 0.190, T_p = 31.3 days, and I_{max} = 4.43%.

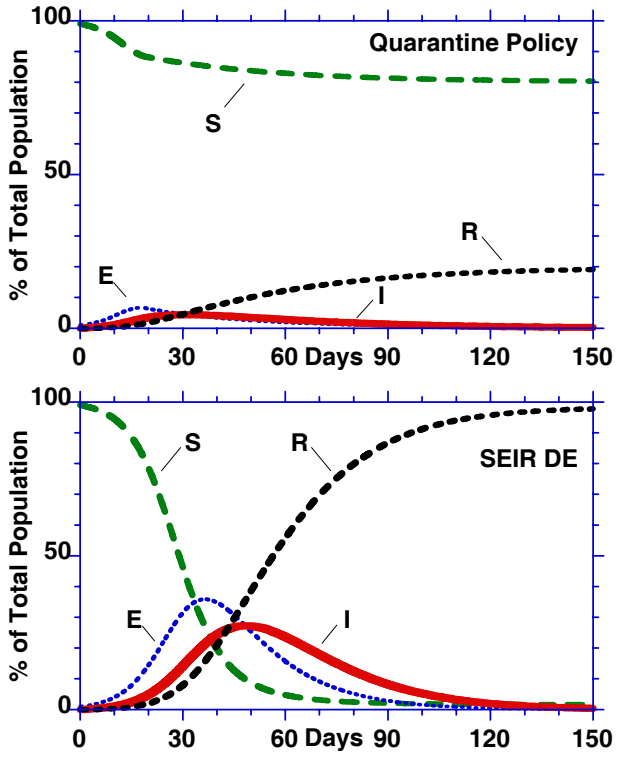

Figure EC.4 DE model behavior under quarantine (top) compared to base case (bottom).

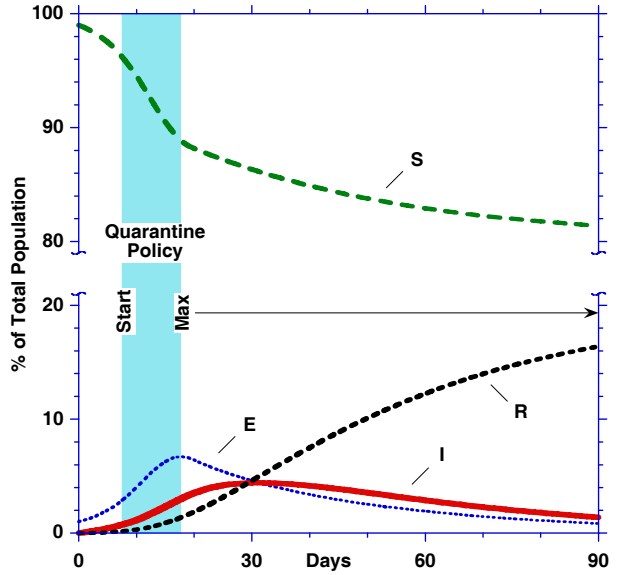

Figure EC.5 First 90 days of the quarantine case in the DE model, showing when the quarantine policy is initiated (around day 8) and when it reaches full implementation (around day 18).

Another important question raised by the policy analysis is whether the differences between the AB and DE models are large relative to the impact of the policy (the change in metrics from the base case to the policy case). The change in a metric such as T_p or F is relevant because it will inform the cost-benefit tradeoffs policymakers face. For example, policymakers may trade off the cost of a policy against the number of cases avoided using some standard for the value of a life, QALY or DALY. To address this question we need to find the change in each metric resulting from the implementation of the policy across different AB scenarios and compare these changes to the change in each metric for the DE case resulting from the implementation of the same policy.

In each AB scenario we have 1000 simulations in the base case and 1000 in the policy case. To assess the change in each metric as a result of policy implementation, we need to create a one-to-one mapping between base case and policy simulations. However, there is no clear one-to-one mapping between these simulations. For example, policy intervention in base simulation *i* could have resulted in multiple policy simulation trajectories depending on the stochastic unfolding of the policy case. Using the same random number seed in the base and policy simulations of the AB model would not solve the problem because the sequence of particular contacts between infectious and susceptible individuals is endogenous and contingent on the impact of the policy.

We estimate the change in each metric arising from the policy in the AB models as follows. Each realization of the AB model in a given experimental condition in the base case (no policy) is compared to a randomly selected realization of the AB model in that same condition in the policy case. The change in the value of each metric ΔT_p, ΔI_{max}, and ΔF is calculated. This is repeated for each of the 1000 AB simulations in each experimental condition. Table EC.7 reports the change in the metrics from the base case to the quarantine case using this procedure.

Change in Metric		Connected		Random		Scale-free		Small World		Lattice	
		$H_{=}$	$H_{\neq}$	$H_{=}$	$H_{\neq}$	$H_{=}$	$H_{\neq}$	$H_{=}$	$H_{\neq}$	$H_{=}$	$H_{\neq}$
Change in Final Size $\Delta F = 0.793$	**Mean**	0.75	0.65	0.77	0.66	0.75	0.59	0.80	0.71	0.54	0.41
	σ	0.15	0.21	0.17	0.19	0.19	0.23	0.18	0.22	0.29	0.26
Change in Peak Time, $\Delta T_p = 16.8$	**Mean**	14.8	8.9	19.7	14.9	11.1	7.8	56.2	53.1	55.0	44.8
	σ	18.8	20.7	20.1	22.2	20.2	22.5	34.7	39.6	59.1	52.4
Change in Peak Prev, $\Delta I_{max} = 22.6$	**Mean**	22.6	19.9	21.3	18.9	21.8	17.9	14.0*	12.2*	5.3**	4.6**
	σ	5.5	6.8	5.5	6.2	6.3	7.3	5.2	5.6	3.7	3.7

Table EC.7 Change in metrics caused by the policy. The table shows the value of the metric in the base case less its value under the policy. */** indicates the change in the value of the metric in the DE model falls outside the 95/99% confidence bound defined by the ensemble of changes in pairs of AB simulations.

The difference between the base and policy values of T_p and F in the DE falls inside the 95% interval of outcomes for all network and heterogeneity conditions. The difference between the base and policy values of I_{max} in the DE falls within the 95% interval for all cases except the small world and lattice. The policy impact is smaller in these conditions than in the DE because the mean of I_{max} in the base-case AB model in these relatively clustered networks is smaller than in the DE. In the base case heterogeneity generally lowers final size compared to the DE because highly connected individuals with high contact frequencies tend to become infected sooner and are therefore removed from the infectious population sooner, lowering the mean contact frequency for the remaining population. In contrast, under contact reduction, heterogeneity tends to increase peak time. At the start of an outbreak the highly connected individuals fuel a quick take-off, increasing the size of the exposed (asymptomatic) population before the first cases are detected and the intervention can quench the epidemic. Consequently heterogeneity leads to higher values of final size. As a result of these two effects, the mean values of ΔF in the heterogeneous cases of the AB model are smaller than the value generated by the DE. However, heterogeneity also increases outcome variability, so the range of outcomes caused by random inter-

actions among members of the population is larger, reducing the practical significance of the differences in policy impact between the DE and AB models.

EC.10. Cost-Benefit Analysis and Policy Sensitivity

While the differences across network types and heterogeneity conditions is generally small compared to the large impact of contact reduction, it is important to consider whether the differences in policy response might change the optimal policy set. Two models may have similar overall base-case dynamics yet respond differently to policies. These differences might then cause a different set of policies to be optimal. For simplicity, suppose that policymakers must select either quarantine or no quarantine as discrete and mutually exclusive choices. Ignoring uncertainty, quarantine will be optimal if its benefits B exceed its costs, C. The text provides an example in which per capita quarantine costs are constant at C and the benefits are linear in avoided cases, $B = b\Delta F$. The per capita benefits of each avoided case would include the value assigned per life (or QALY or DALY), the monetary value of avoided health care costs and economic losses arising from loss of tourism and business travel, disruptions to economic output and supply chains, and so on.[7] In this simple example, quarantine would be optimal if $\Delta F > C/b$. As shown in Table EC.7, the values of ΔF vary by network type and heterogeneity condition. For example, in the scale-free case, ΔF is 0.75 for $H_=$ and 0.59 for $H_{\neq}$. Assuming there are no other sources of uncertainty, the quarantine policy is optimal if $C/b < 0.59$ and no quarantine is optimal if $C/b > 0.75$, independent of heterogeneity condition. However, for $0.59 \leq C/b \leq 0.75$, the optimal policy depends on whether the population is characterized by the $H_=$ or $H_{\neq}$ conditions: in such a case the choice of model could have a large impact on policy.

Considering the range of outcomes across all network types and heterogeneity conditions shown in Table EC.7, including the DE, quarantine is optimal if $C/b < 0.41$ and no-quarantine is optimal if $C/b > 0.80$. Between these values the optimal policy depends on which network and heterogeneity condition is judged most likely. To further complicate matters, the values of ΔF

[7] In reality the economic costs of disruption and lost business are likely to be nonlinear: the small number of SARS cases in Toronto did not significantly depress travel and economic activity to the city, while the larger outbreaks in Hong Kong and Taiwan triggered large losses for the tourism and travel industries and substantial disruption to businesses. These social reactions are strongly conditioned by positive feedback processes including panic and bandwagon effects and are thus difficult to estimate.

used in these illustrative calculations are the means over the ensemble of 1000 AB realizations in each condition. As seen in Table EC.7, there is substantial variability in the values of ΔF within each condition. The mean of the standard deviations across all conditions is 0.21, so that the 2σ range of variability in policy impact is roughly equal to the width of the region in which policy is contingent on network type and heterogeneity condition ($2\sigma = 0.42 \approx 0.80\text{-}0.41$). Further, the values of ΔF will also vary over the range of uncertainty in parameters and model boundary. Proper procedure would be for policymakers to construct the probability distribution characterizing the likelihood of each value of ΔF as it depends jointly on all sources of uncertainty, including network topology, individual heterogeneity, parameters such as R_0, the strength of social and behavioral feedbacks, the costs of policy implementation and the benefits of avoided cases, then select whether to implement the policy based on their tolerance for Type I and Type II error. In practice, of course, such decision analysis is not done. Nevertheless, the results show that policy choice can depend on the choice of model even when the base case behavior of the models is similar. If policymakers judge that the parameters are such that the optimal policy is contingent on model choice, then they should allocate additional resources to further empirical work designed to resolve the uncertainty. To make that choice rationally requires that the value of information regarding all sources of model uncertainty be estimated through sensitivity analysis, including analysis over network type, individual variability, model boundary, and so on. The combinatorial explosion in the dimensionality of the required sensitivity analysis forces modelers and policymakers to make tradeoffs imposed by limited time, budget, and computational resources. Carrying out a full sensitivity analysis over policies, parameter uncertainty, network and individual heterogeneity conditions, model boundary, and cost and benefits in an agent-based model with realistic population size is infeasible. A more complete analysis can be carried out in the computationally efficient DE, except that the DE, with its assumptions of homogeneous individuals and perfect within-compartment mixing cannot be used to test the impact of different network topologies and degrees of individual heterogeneity, unless it is disaggregated to include additional compartments representing different types of individuals, locations in the contact network, or other attributes.

Do calibrated DE models offer an efficient compromise? As shown in Tables EC.1 and EC.2, the calibrated DE model fits individual realizations of the AB model well even though it does not explicitly capture network clustering or individual heterogeneity. If the response of the calibrated models to policy interventions is also similar to that of the AB models, then policy-makers could use the computationally efficient calibrated DE models to explore policy impacts, and, for any given budget and time frame, could carry out more sensitivity analysis than would be possible in the computationally intensive AB model.

To test this hypothesis we conducted the following experiment. We simulated the contact reduction scenario in the DE model for every calibrated case (200 parameter sets in each of the ten experimental conditions). In each, the contact rate was modeled using equations 6-7 in the paper. The goal of this comparison is to determine whether the policy response of the calibrated DE models is similar to the policy response of the AB models for the purpose of assessing the impact of alternative policy interventions. Other purposes could also be considered, for example, forecasting the progression of an epidemic, designing studies to reduce uncertainty in key parameters or test theories about modes of transmission, etc. Here we test whether the good fit of the calibrated DE models to the AB model outcomes implies that the policy response of the two model types will be similar. Table EC.8 reports the results.

Metric		Connected		Random		Scale-free		Small World		Lattice	
		$H_=$	$H_{\neq}$	$H_=$	$H_{\neq}$	$H_=$	$H_{\neq}$	$H_=$	$H_{\neq}$	$H_=$	$H_{\neq}$
Final Size F (0.190)	μ	***0.212***	0.105	0.111	0.075	***0.112***	0.061	***0.135***	***0.083***	***0.064***	***0.047***
	σ	0.122	0.041	0.040	0.030	0.044	0.026	0.054	0.034	0.040	0.025
Peak Time T_p (31.3)	μ	***32.98***	24.39	28.14	22.63	30.81	18.19	42.60	36.73	32.76	24.43
	σ	7.42	6.57	5.53	7.42	7.46	7.84	11.90	15.12	23.04	19.20
Peak Prev I_{max} (4.43)	μ	4.35	3.41	3.27	2.74	3.02	2.61	2.65	2.19	1.75	1.72
	σ	1.53	0.95	0.88	0.77	0.81	0.77	0.74	0.65	0.49	0.48

Table EC.8 Results of contact reduction in the calibrated DE models. Base DE values are reported in parentheses. The results should be compared with the Table EC.6, which reports the same metrics for the corresponding AB simulations. Mean values in ***italics*** show cases in which the calibrated DE provides a better fit to the AB means than the uncalibrated base case DE.

Comparing the results in tables EC.8 and EC.6 shows that, after application of the policy, the DE models using the calibrated parameter values fail to show a high correspondence to the corresponding AB simulations. The calibrated DE models provides a better fit to the mean of the AB realizations for F and T_p in the homogeneous connected case, and I_{max} is nearly the same in the calibrated and base cases. This is expected since the connected case is closest to the DE model assumptions; differences among individual realizations reflect only the stochastic variation induced by random interpersonal contacts. In the heterogeneous connected case, however, the uncalibrated base DE parameters provide a better fit to the mean of the AB realizations than the calibrated models. Across the other conditions, the mean of the calibrated models provides a better fit to the mean of the AB realizations only for F in the small world and lattice networks, and in the $H_=$ scale free condition. The base model outperforms the mean of the calibrated models in all conditions for T_p and I_{max} (except as noted, for T_p in the $H_=$ connected case). The calibrated parameter values that successfully captured the network and heterogeneity effects in the base case fail to capture those effects in the policy simulation.

The results show that the ability of the simple four-compartment deterministic SEIR model to capture the base case behavior of individual AB epidemics does not imply that these simple models can be used to assess the impact of policies. Further work is needed to explore the implications. Specifically, additional studies are required to determine the extent to which the results arise from violations of the mixing and homogeneity assumptions vs. the stochastic variation in individual realizations (Tables 3-4 and Figure EC.3 suggest both play a role). Additionally, further work is required to determine whether disaggregating the DE models into more compartments to capture key aspects of clustering and heterogeneity might improve the results, and how AB simulation results might be used to find optimal partitions in such models.

EC.11. Simulating the model

Two versions of the model are posted with the online material. Both are developed in the Anylogic ™ software. Anylogic supports both agent-based and differential equation models. One interface is a stand-alone Java applet and runs under any Java-enabled browser with no need to install additional software. The second includes the source code and equations of the model

and can be used for detailed inspection of model implementation and for simulation, once the Anylogic software is installed.

To open the stand-alone applet, unzip "ABDE-Contagion-applet.zip" into one folder (all three files need be in the same folder). You can then open the "Dynamics of Contagion_Apr05_Paper Applet.html" file in any web browser (e.g. Internet Explorer). The interface is self-explanatory and includes a help file, which can be opened by clicking the [?] button.

To open the Anylogic model source code, download and install the Anylogic software (a free 15-day trial is available at http://www.xjtek.com/download/). Unzip the attached file "ABDE-Contagion-code.zip" in one folder. Open the file "Dynamics of Contagion_Apr05_Paper.alp" in Anylogic. The list of all objects in the agent-based model is displayed in the left hand column; select any object to inspect its formulation. Run the model by clicking on the run button (or pressing F5), which compiles the model and brings up an interface similar to the Java applet. You can inspect the behavior of the model both through the interface accompanying the model and applet, or by browsing different variables and graphing them in Anylogic run mode. To do the latter, go to "root" tab in run time mode, where you can see all model variables and can inspect their runtime behavior.

The implemented interface allows users to:

1. Run the model for different scenarios in single or multiple runs.
2. Inspect the behavior of the AB model, including the number of people in each state, state transition rates and user-specified confidence intervals for the infected population.
3. Visually inspect diffusion of the epidemic in the network. Different nodes and links between them are shown. You can choose among 4 different representations of the network structure to show the progression of the epidemic through the network.
4. Observe the metrics of peak value, peak time, and final size.
5. Change model parameters, including the incubation and recovery periods, infectivities, and contact rates (note that mean contact rates for exposed and infected individuals are expressed as fractions of the contact rate for healthy individuals). You can also set the size of the population, network type, number of links per person, and probability of long-range links in small-world network, and select the heterogeneous or homogeneous condition.
6. Save the results into a text file for subsequent analysis.

References

Anderson, R. M. and R. M. May 1991. *Infectious diseases of humans dynamics and control.* Oxford University Press, Oxford.

Barabasi, A. L. and R. Albert. 1999. Emergence of scaling in random networks. *Science* **286** (5439) 509-512.

Fahse, L., C. Wissel and V. Grimm. 1998. Reconciling Classical and Individual-Based Approaches in Theoretical Population Ecology: A Protocol for Extracting Population Parameters from Individual-Based Models. *The American Naturalist* **152**(6) 838-852.

Newman, M. 2003. Random graphs as models of networks. *Handbook of graphs and networks*. S. Bornholdt and H. G. Schuster, eds. Berlin, Wiley-VCH**:** 35-68.

Wallinga, J. and P. Teunis. 2004. Different epidemic curves for severe acute respiratory syndrome reveal similar impacts of control measures. *American Journal of Epidemiology* **160** (6) 509-516.

Watts, D. J. and S. H. Strogatz. 1998. Collective dynamics of "small-world" networks. *Nature* **393**, 440-442.